Analysis of a magnetically trapped atom clock

D. Kadio[1] and Y. B. Band[1,2]
[1]*Departments of Chemistry and Electro-Optics, and The Ilse Katz Center for Nano-Science, Ben-Gurion University of the Negev, Beer-Sheva 84105, Israel*
[2]*Atomic Physics Division, A267 Physics, National Institute of Standards and Technology, Gaithersburg, Maryland 20899, USA*
(Received 8 May 2006; revised manuscript received 15 September 2006; published 8 November 2006)

We consider optimization of a rubidium atom clock that uses magnetically trapped Bose condensed atoms in a highly elongated trap, and determine the optimal conditions for minimum Allan variance of the clock using microwave Ramsey fringe spectroscopy. Elimination of magnetic field shifts and collisional shifts are considered. The effects of spin-dipolar relaxation are addressed in the optimization of the clock. We find that for the interstate interaction strength equal to or larger than the intrastate interaction strengths, a modulational instability results in phase separation and symmetry breaking of the two-component condensate composed of the ground and excited hyperfine clock levels, and this mechanism limits the clock accuracy.

DOI: 10.1103/PhysRevA.74.053609 PACS number(s): 03.75.Nt, 03.75.Kk, 03.75.Mn, 06.30.Ft

I. INTRODUCTION

The most accurate atomic clocks in operation today are based either on trapped single ions or on atomic beams. The advantage of ion clocks is that a single ion can be trapped very tightly by static electric fields such that optical transitions do not cause significant heating or an escape of the ion. These optical transitions are decoupled from the trapping potential such that both ground and excited atomic states feel the same potential. On the other hand, one advantage of atomic beam clocks is the large number of atoms in a beam, such that the quantum projection noise can be decreased by 2–3 orders of magnitude with respect to the single ion clock. A clock based on a thermal atomic beam suffers from the velocity distribution that limits the transition bandwidth. Using a Bose-Einstein condensate (BEC) would significantly ameliorate this problem. A new type of atomic clock based on neutral atoms trapped in a deep "magic-wavelength" optical lattice (magic because the transition does not have an optical light shift because the difference between the ac polarizabilities vanishes at the wavelength of the optical lattice) has recently been suggested [1,2]. This kind of clock can be operated on an optical transition, rather than a microwave transition, and promises to be most accurate, but clocks of this type have not yet been fully characterized.

Here we consider whether a good atomic clock can be based on a more common type of trapped ultracold atom configuration, i.e., on a BEC in a magnetic trap. Trapped BECs can have many atoms, which gives them the large number advantage mentioned above. This kind of clock can be much more accurate than a thermal cloud clock because the Doppler effect in a thermal clould can severely limit clock performance (see Sec. III B below). This effect is negligible for a BEC. In addition a BEC cloud has a well-defined energy determined by the chemical potential that is uniform over the BEC and this helps in lowering the variance of the clock frequency. This kind of clock might be miniaturized, as microtraps for atomic BECs can be created above a fabricated chip. As has now been fully demonstrated, magnetic microchip traps can be used to manipulate neutral atoms on the micrometer scale [3]. A high density, coherent atom source can be created via Bose-Einstein condensation on an atom chip [4], and "atomic conveyor belts," waveguides, and beam splitters can be implemented on atom chips [3]. It is therefore intriguing to entertain the possibility of creating an atomic clock on an atom chip [5,6]. Hence, it is important to study theoretically and experimentally the potential of this kind of clock. One experiment of this kind, using Ramsey spectroscopy [7], has already been carried out [5], and another experiment has been performed in a macroscopic magnetic trap [8], but using the same spectroscopic method. More recent mesoscopic atom clocks using coherent population trapping have been reported [6], and have the benefit of allowing compact optical light sources.

Specifically, we consider a BEC in a magnetic trap and investigate a clock based on the Ramsey separated field spectroscopy method [7] in a highly elongated trap. The quasi-1D geometry of an elongated trap has the advantage of further reducing the inelastic ultracold collisions as shown in Ref. [9]. As in Refs. [5,8], we consider a two-photon microwave transition between two ^{87}Rb hyperfine states with an atomic frequency $\nu_0 \simeq 6.8$ GHz. We treat the dynamics of the clock in mean field and consider the amplitude and phase of the order parameters for the ground and excited clock states of the system, solving the coupled set of one-dimensional (1D) Gross-Pitaevskii equations to analyze the microwave clock frequency shift due to collisional and magnetic field effects. We determine the clock frequency shift introduced by the external magnetic potential and the kinetic energy of the Bose condensed gas, both of which are influenced by the difference in the size of the two atomic wave packets. The clock is designed to run with ^{87}Rb atoms in a magnetic field regime where the two hyperfine levels correlating with $5\,^1S_{1/2}|f=1,m_f=-1\rangle$ and $5\,^1S_{1/2}|f=2,m_f=1\rangle$ experience the same first-order Zeeman shift [5,8,10]. The collisional frequency shift from the resonance frequency ν_0 can be calculated as in Ref. [8]. As we shall see, the collisional shift can be cancelled by using the Zeeman shift [8] and by optimizing the population difference in the ground and excited states [11]. The latter is possible for an interstate interaction strength larger or smaller than both the ground and excited intrastate interaction strength. The clock run time is limited by atom loss due to collisional spin dipolar collisional relaxation of the excited state [8]. For a ^{87}Rb condensate at high

density (12.6×10^{13} cm^{-3}), the collisional dipolar loss in the excited state has been experimentally measured [8]. Atom loss led to a total density to drop by 3% in 20 ms. Nevertheless it is important to have a reasonable atomic number density n to compensate the effects of quantum fluctuations; the uncertainty, as quantified by the Allan standard deviation σ scales as $n^{-1/2}$. So an optimization of the density of atoms is necessary to reduce the quantum fluctuations and the collisional dipolar relaxation in order to increase the clock time. The first experiment with this type of clock using a trapped thermal cloud of ^{87}Rb atoms containing about 1.5×10^4 atoms with a density of atoms less than 5×10^{12} cm^{-3}, yielded an Allan standard deviation

$$\sigma(\tau) = 1.7\times10^{-11}\tau^{-1/2}\ \mathrm{Hz}^{-1/2}, \tag{1}$$

where τ is the averaging time [5]. For the trap parameters used here, i.e., with radial frequency $\omega_r/2\pi=120$ Hz and axial frequency $\omega_z/2\pi=0.5$ Hz, the Allan standard deviation is of order of magnitude $10^{-12}\sqrt{T_c/\tau}$, where T_c is the cycle period. This trap confines the geometry to quasi-1D and has the advantage of further reducing the collisional dipolar relaxation [9].

Some additional crucial limitations might make a magnetically trapped BEC unsuitable. A significant limitation is the collisional interaction between the atoms. Particularly problematic is the difference in the s-wave scattering length between atoms occupying different hyperfine levels which affects the collisional shift of the clock frequency. The collisional shifts of rubidium atoms are relatively small compared to cesium atoms [12,13], for example, but they can still be significant if many atoms are tightly trapped together. In order to minimize collisional shifts, we shall employ a method of overcoming collisional shifts by adjusting the ground to excited state ratio during the Ramsey fringe spectroscopy. Moreover, the run time of the clock is also limited by the dynamics of the atomic cloud that can result in phase separation of the two spin components [14–18]. We find that a *modulational instability* results in the dynamics and the evolution depends on both the density of atoms and the balance between the interstate and intrastate interaction strengths. This gives rise to phase separation and symmetry breaking of the two-component condensate for the ground and excited clock levels that occurs after the first $\pi/2$ Ramsey pulse that puts the atoms in a superposition of the ground and excited state. The modulation instability limits the clock accuracy. It therefore appears that magnetically trapped BEC clocks on an atom chip cannot promise to be the most accurate type of clock. The most significant limitation to the clock stability arises from the dynamics of the atomic cloud that creates a phase separation of the two wave packets for the ground and excited state. The time dependence of the phase separation depends on the density of atoms and on the interstate interaction strength; the smaller the density and/or the smaller the interstate interaction strength, the longer the phase separation time. Hence, a very weak axial trapping frequency (e.g., $\omega_z/2\pi<0.5$ Hz) resulting in a lower density of the atoms, allows an increased interrogation time and/or a greater total number of atoms, and therefore a further increase of the stability of the clock beyond $10^{-12}\sqrt{T_c/\tau}$.

The paper is organized as follows. The model of the clock based on Ramsey spectroscopy is described in Sec. II. Section III A briefly presents the numerical approach we use to analyze the clock. In Sec. III B we depict the quasi-1D dynamics in a trap that is very tight in two directions, and describe why the spin-relaxation collision mechanism, as well as other inelastic scattering processes, is suppressed in a 1D geometry. Section III C describes the results obtained by numerically solving the coupled Gross-Pitaevskii equations for the order parameters of the ground and excited clock states. In Sec. IV we discuss two ways to improve and optimize the stability and accuracy of the clock by cancelling the collisional shift. Section V concludes the paper.

II. MICROWAVE BEC MAGNETIC CLOCK USING RAMSEY FRINGES

We consider an atomic BEC trapped in an external magnetic potential. The spatial variation is harmonic about the trap minimum. The atoms are initially in the ground electronic state, labeled $|1\rangle$, and a radio-frequency field can transfer atoms into an excited state labeled $|2\rangle$. More specifically the levels $|f,m\rangle=|2,1\rangle$ and $|1,-1\rangle$ are used, and the transition involves a combination of a microwave pulse at 6.8 GHz to transfer the atoms from $|2,1\rangle$ to $|1,0\rangle$ and then another RF pulse to transfer them from $|1,0\rangle$ to $|1,-1\rangle$. The $|1,-1\rangle$ state is trapped with the same potential as $|2,1\rangle$ if the magnetic field at the trap bottom is around 3.23 G [10].

The clock described here uses the Ramsey separated field method [7]. The atomic cloud interacts with two short microwave pulses separated by a time T; each pulse has pulse area close to $\pi/2$. A spatial inhomogeneity of the atomic energy levels is due to the spatially dependent Zeeman energy due to the magnetic field varying with position. Clearly, this can adversely affect the clock frequency. This effect is minimized by using a pair of energy levels which experience the same trapping potential at a particular magnetic field strength. References [5] and [8] showed that at a magnetic field of $\sim$3.23 G, the $|1\rangle\equiv|f=1,m_f=-1\rangle$ and $|2\rangle\equiv|f=2,m_f=1\rangle$ hyperfine levels of the $5S_{1/2}$ ground state of ^{87}Rb experience the same first-order Zeeman shift such that the differential shift of the two levels across the cloud was $\sim$1 Hz. The collisional shift also contributes to the spatial inhomogeneity of the atomic transition energy level across the cloud since the density of the cloud varies with position. However, as noted in Ref. [8], it may be possible to cancel the Zeeman shift with the collisional shift. The stability and accuracy of the clock are further improved and optimized by cancelling the collisional shift (as we shall see in Sec. IV).

The initial condensate starts in the ground state $|1\rangle$, and after the first $\pi/2$ pulse, which we model by Bloch sphere dynamics [19] assuming that the pulse duration τ_p is extremely fast compared to other time scales, we solve a set of coupled Gross-Pitaevskii equations to describe the dynamics of the two-component ($|1\rangle$ and $|2\rangle$) wave packets. After a time T a second short $\pi/2$ pulse is applied. For an intense short near-resonant pulse, the solutions of the optical Bloch equations for a two level atom gives the following unitary transformation operator:

$$\mathbf{U}(t) = \begin{pmatrix} \cos(\Omega_g t/2) - i\frac{\Delta\nu}{\Omega_g}\sin(\Omega_g t/2) & -i\frac{\Omega}{\Omega_g}\sin(\Omega_g t/2) \\ -i\frac{\Omega}{\Omega_g}\sin(\Omega_g t/2) & \cos(\Omega_g t/2) + i\frac{\Delta\nu}{\Omega_g}\sin(\Omega_g t/2) \end{pmatrix}, \tag{2}$$

where Ω is the Rabi frequency, $\Delta\nu$ is the detuning and $\Omega_g = \sqrt{|\Omega|^2 + \Delta\nu^2}$ is the generalized Rabi frequency. For example, if an atom is initially in state $|1\rangle$ and interacts with an on-resonant $\pi/2$ pulse, it evolves to the state $(|1\rangle + i|2\rangle)/\sqrt{2}$. This transformation can be used to describe the effects of both the first and second Ramsey pulses.

III. MEAN-FIELD ANALYSIS OF CLOCK DYNAMICS

The performance of the clock is affected by the dynamics of the two-component BEC after the first $\pi/2$ Ramsey pulse. We shall see below that, because of the crossed interaction energy of the two spin components created after the first $\pi/2$ Ramsey pulse, the system becomes unstable, and the components eventually undergo a local phase separation that leads to symmetry breaking. The phase separation of the spin components limits the Ramsey interrogation time and hence the stability of the clock.

In this section, we first describe the numerical methods used to investigate the clock dynamics in mean field. Many-body effects can also be included as formulated in Ref. [20], but we shall not do so here. Then we discuss the advantage of operating the clock in a highly elongated trap configuration. We present numerical results for this configuration and analyze them.

A. Numerical method

We investigate the clock dynamics in mean field. The initial zero temperature condensate wave function (order parameter) is obtained by numerically determining the lowest eigenstate $\psi(\mathbf{r})$ of the time-dependent Gross-Pitaevskii equation for particles of mass m, confined in an external potential $V_{\text{ext}}(\mathbf{r})$ and a mean-field interaction energy due to contact two-body interactions with coupling strength $g_{11} = 4\pi\hbar^2 a_{11}/m$ where a_{11} is the s-wave scattering length for atoms in the ground state. This is accomplished with an imaginary time split-step Fourier transform method. The effect of the first pulse that couples the two atomic spin states is modeled using a unitary transformation on the zero temperature ground state wave function and gives two wave functions representing the ground state and the excited state atoms:

$$\psi_i(\mathbf{r},0) = A_i\psi(\mathbf{r}), \tag{3}$$

where $i=1,2$ correspond to ground and excited state labels, respectively, and A_i is the complex amplitude of state i obtained using Eq. (2). We take the normalization of the initial condensate wave function such that $\int|\psi(r,0)|^2 d\mathbf{r} = N$, where N is the total number of atoms, and the amplitudes A_i are determined by the Bloch sphere dynamics for the two levels in the presence of the microwave field inducing the transition [19]. The amplitudes A_i satisfy $0 \leq |A_i|^2 \leq 1$ and $\Sigma_{i=1}^2 |A_i|^2 = 1$. The two component condensates evolve according to

$$i\hbar\frac{\partial\psi_i(\mathbf{r},t)}{\partial t} = \left(-\frac{\hbar^2\nabla^2}{2m} + V_{\text{ext}}(\mathbf{r}) + (-1)^i\frac{\hbar\omega_{21}}{2} + \sum_{j=1,2} g_{ij}|\psi_j(\mathbf{r},t)|^2\right)\psi_i(\mathbf{r},t), \tag{4}$$

where the atomic resonance transition frequency is denoted as ω_{21}. The interaction strength $g_{ij} = 4\pi\hbar^2\alpha_{ij}^{(2)}a_{ij}/m$, with $i,j=1,2$, is defined in terms of the s-wave scattering length for particles in states i and j, a_{ij}, and the two-particle correlation parameter for particles in states i and j at zero separation between particles, $\alpha_{ij}^{(2)}$ [8,21–25]. The latter quantity is often denoted as $g_{ij}^{(2)}$. The values of the two-particle correlation parameter $\alpha_{ij}^{(2)}$ is such that $0 \leq \alpha_{ii}^{(2)} \leq 2$ and $1 \leq \alpha_{ij,i\neq j}^{(2)} \leq 2$ for bosons. For a condensate, $\alpha_{ii}^{(2)} = 1$. For the interstate (two-component) two-particle correlation at zero separation, $\alpha_{12}^{(2)}$ in a condensate we considered two values, $\alpha_{12}^{(2)} = 1$ and $\alpha_{12}^{(2)} = 2$. We have learned recently that $\alpha_{12}^{(2)}$ was measured to be nearly unity for ^{87}Rb [26], but to we shall present results of calculations for both values.

We propagate the two BEC components for a time T between the Ramsey pulses by solving the coupled time-dependent Gross-Pitaevskii equations using the split-step Fourier transform method. During the propagation for a time T, the phase and amplitude of the component wave functions evolve with time. After the time T, we apply again the unitary transformation operator corresponding to a $\pi/2$ pulse. We then integrate the component wave functions over space to obtain the probabilities for finding the atoms in the two states.

B. Dynamics of the clock in a highly elongated trap

The effects of the mean-field collisional dipolar relaxation are important to investigate in order to optimize the accuracy and the stability of the clock. As we shall see, phase separation of the two spin components due to mean-field dynamics, and loss of excited state atoms due to the collisional dipolar relaxation between atoms in the excited state are two factors that can significantly reduce the performance of the clock. The collisional dipolar loss of the excited state for a ^{87}Rb condensate at high density (12.6×10^{13} cm^{-3}) has been experimentally measured [8]. Atom loss caused the total density to drop by 3% in 20 ms. In order to reduce this effect, we propose to run the clock in a highly elongated trap; in a

quasi-one-dimensional condensate the spin-dipole relaxation collisional loss can be made much smaller than in three dimensions [9]. The inelastic rate coefficient for going from the incident channel β to a final inelastic channel β' for strong confinement $K_{\mathrm{conf},\beta'\beta}$ is related to the 3D inelastic rate $K_{\mathrm{free},\beta'\beta}$ by [9],

$$K_{\mathrm{conf},\beta'\beta} = \frac{a_\perp^4 p_0^2}{4\hbar^2 |a_{\mathrm{eff}}|^2} K_{\mathrm{free},\beta'\beta} = \frac{2\pi a_\perp^4 E_0}{\hbar^2} \sum_{\beta'} \frac{|U_{\beta'\beta}|^2}{p_{\beta'}}. \quad (5)$$

Here p_0 is the relative collision momentum and $E_0 = p_0^2/2\mu_r$ is the relative collision energy in the incident channel, $p_{\beta'} = \sqrt{2\mu_r(E_0 + E_{\beta'\beta})}$ is the relative momentum in the final inelastic β' channel, where $E_{\beta'\beta}$ is the asymptotic energy difference of the two channels, $\mu_r = m/2$ is the reduced mass, and the parameter $U_{\beta'\beta}$ is the coupling between the channels β' and β. This quasi-1D rate is reduced by a factor of $\frac{a_\perp^4 p_0^2}{4\hbar^2 |a_{\mathrm{eff}}|^2}$ from the 3D rate, and is small for ultracold collision energies. For high anisotropy of the trap, the 1D interaction strength is given by

$$g_{ij}^{1\mathrm{D}} = \frac{2\hbar^2 \alpha_{ij}^{(2)} a_{ij}}{m a_\perp^2}, \quad (6)$$

where $a_\perp = \sqrt{\hbar/m\omega_r}$ is the radial harmonic oscillator length and $\omega_r/2\pi$ the radial trap frequency [27]. For sufficiently large ω_r, radial profile is harmonic oscillatorlike, and the motion of the atoms are frozen in the radial direction. We assume that the magnetic field is such that the first-order Zeeman shift is the same for the two atomic internal states. Now, if the frequency $\omega_z/2\pi$ is also made small, so the 1D density is small, the nonlinear interaction term $g_{ij}^{1\mathrm{D}} n$ can be made very small.

Using a magnetically trapped thermal cloud can significantly reduce the mean-field collisional shift compared to a BEC, however, a thermal cloud has a Doppler width that increases the bandwidth of the clock transition and can therefore limit the clock accuracy. Indeed the clock bandwidth at half-maximum is in our case inversely proportional to the interrogation time T; the larger the interrogation time, the smaller the transition bandwidth of the clock, and the Doppler effect on the bandwidth becomes more significant. With our interrogation time (0.5 s), the Doppler width must be much smaller than 1 Hz to be negligible. Hence, the temperature of the thermal cloud must be well below 2.5 μK so as to be competitive with a BEC. For a 500 nK ^{87}Rb thermal cloud (i.e., above condensation) the Doppler width is 0.4 Hz which is smaller than the bandwidth of the clock transition. Moreover, in a BEC the energy is determined by the chemical potential that is uniform across the BEC and very well specified; this helps in lowering the variance of the clock frequency. The collisional frequency shift calculated with 10^4 atoms in a highly elongated BEC corresponding to a density of 3×10^{14} atoms/cm^3 for our trap geometry, is about 3 Hz, but the uncertainty in this collisional shift (due to the uncertainty in the number of atoms and the uncertainty in the value of the scattering length) is very much smaller than 3 Hz, and hence the collisional shift can be largely compensated for as far as the clock frequency is concerned. Although the collisional shift for a 500 nK thermal cloud is at least 100 times smaller than that for the BEC, the Doppler width of the thermal cloud is 0.4 Hz, and this is presumably much larger than the *uncertainty* in the collisional shift of the BEC.

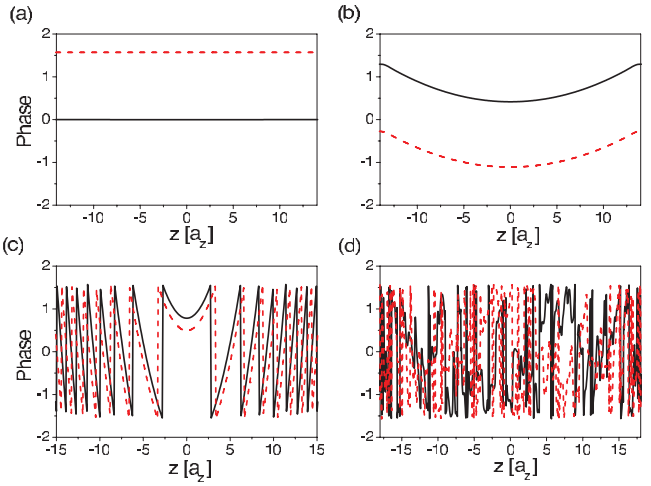

FIG. 1. (Color online) Phase of condensate ground state (solid curve) and excited state (dashed curve) components for the interstate two-particle correlation parameter at zero separation $\alpha_{12}^{(2)}=2$, after the first $\pi/2$ pulse as a function of position, z, in the magnetic trap at times (a) $t=0$ ms, (b) $t=6.3$ ms, (c) $t=180$ ms, and (d) $t=500$ ms. $a_z=\sqrt{\hbar/m\omega_z}$ is the axial harmonic oscillator length.

C. Numerical results

Our numerical calculations have been carried out with an axial (ν_z) and radial (ν_r) trap frequency of 0.5 Hz and 120 Hz, respectively, so the anisotropy ratio $\lambda \equiv \nu_r/\nu_z = 240$. The three scattering lengths are taken to be $a_{11}=100.44a_0$, $a_{22}=95.47a_0$, and $a_{12}=98.09a_0$ [8], where a_0 is the Bohr radius. In order to better understand the effect of the modulational instability on the clock, we carry out the calculation with $\alpha_{11,22}^{(2)}=1$ and $\alpha_{12}^{(2)}=2$. The optimization of the number of atoms for the frequencies given above that gives the best Allan deviation is of the order of magnitude 10^4 atoms. The two pulses used for the Ramsey separated field method are taken to be $\pi/2$ pulses, i.e., $|A_1|^2=|A_2|^2=1/2$.

Figure 1 shows the phase $\theta_i(z,t)$ of the ith condensate wave function, $\psi_i(z,t)=|\psi_i(z,t)|\exp[i\theta_i(z,t)]$, as a function of position, z, in the magnetic trap for $\alpha_{12}^{(2)}=2$. Immediately after the first $\pi/2$ pulse, the phase of the two spin components is spatially uniform and their difference is $\pi/2$ [Fig. 1(a)] as is easily understood from the transformation in Eq. (2). Following the $\pi/2$ pulse, mean-field effects begin to create a spatially varying phase across the two condensate wave packets [Figs. 1(b) and 1(c)] [28]. Beyond $t=0.24$ s, the spatially dependent variations in the phase appears completely chaotic; the mean-field treatment has not only reached the point of numerically limited accuracy but has actually lost its regime of validity.

Figure 2 shows the evolution of the position dependent density of the two atomic states for a sequence of interpulse times $T=0$ s [Fig. 2(a)], $T=0.18$ s [Fig. 2(b)], $T=0.22$ s [Fig.

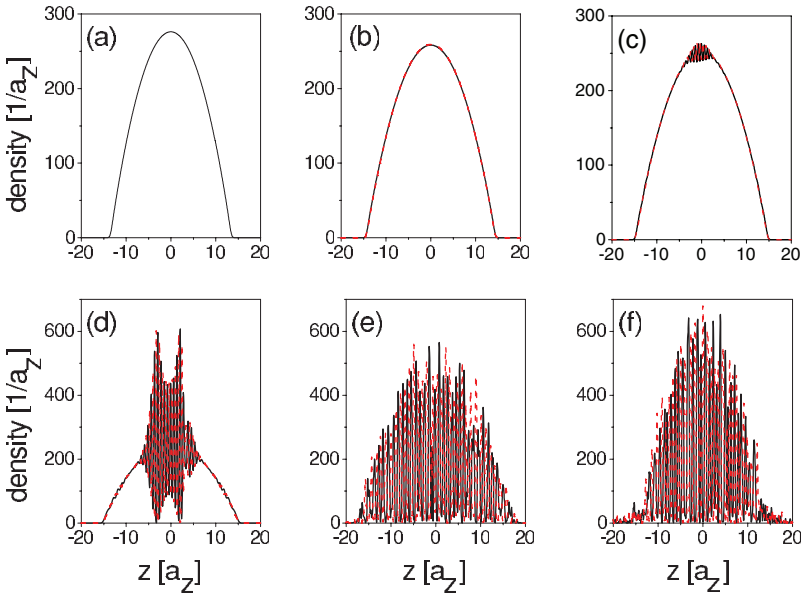

FIG. 2. (Color online) Condensate density of ground state (solid curve) and excited state (dashed curve) components for the interstate two-particle correlation parameter at zero separation $\alpha_{12}^{(2)}=2$, after the first $\pi/2$ pulse for a sequence of interpulse times (a) $T=0$ s, (b) $T=0.18$ s, (c) $T=0.22$ s, (d) $T=0.26$ s, (e) $T=0.5$ s, and (f) $T=1$ s. At $T=0$ s the two spin components have the same amplitude since the microwave pulse is very short but dephased of $\pi/2$ for a $\pi/2$ pulse. $a_z=\sqrt{\hbar/m\omega_z}$ is the axial harmonic oscillator length.

2(c)], $T=0.26$ s [Fig. 2(d)], $T=0.5$ s [Fig. 2(e)], and $T=1$ s [Fig. 2(f)], and $\alpha_{12}^{(2)}=2$. The density of the two components are almost identical at $T=0$ s and $T=0.18$ s and are smoothly varying with position. The density profiles begins becoming irregular at the center of the condensates at about $T=0.20$ s. At later times a spiked structure whose amplitude increases with time develops and some local phase separation occurs [Figs. 2(c)–2(f)] due to the repulsive interaction between the wave packet components. A similar spiked structure of the density as a function of position has been obtained numerically in the regime of strong excitation of the BEC loaded in a 1D optical lattice plus an asymmetric external magnetic trap by instantaneously giving a large displacement to the initial position of the center of the magnetic trap in Ref. [29].

The dynamics is different for $\alpha_{12}^{(2)}=1$. Figure 3 shows the evolution of the position dependent density of the two atomic states for a sequence of interpulse times $T=0$ s [Fig. 3(a)], $T=0.36$ s [Fig. 3(b)], $T=1$ s [Fig. 3(c)], $T=2$ s [Fig. 3(d)], $T=50$ s [Fig. 3(e)], and $T=220$ s [Fig. 3(f)]. The phase separation appears later, around 0.4 s, and evolves more slowly than the case of strong interstate interaction strength ($\alpha_{12}^{(2)}=2$). Since the interaction strength of the ground state is larger than in the excited state, the ground state density protrudes beyond the excited state density ($T=1$ s), and at later times the phase separation evolves in a complex way under the effect of the instability ($T=2$ s and 50 s) and eventually a symmetry breaking occurs ($T=220$ s).

A rough estimate of the time scale at which the system becomes sensitive to the phase-separation instability, τ_{ps}, can be obtained by using the expression derived by Timmermans in Ref. [17] for a homogeneous system,

$$\tau_{\mathrm{ps}}=2\pi/|\Omega_{-,k_f}|=2\pi\hbar/m|c_-|^2, \tag{7}$$

where

$$\Omega_{-,k}^2=c_-^2k^2+(\hbar k^2/2m)^2 \tag{8}$$

is the dispersion of the double condensate excitation, and the parameter

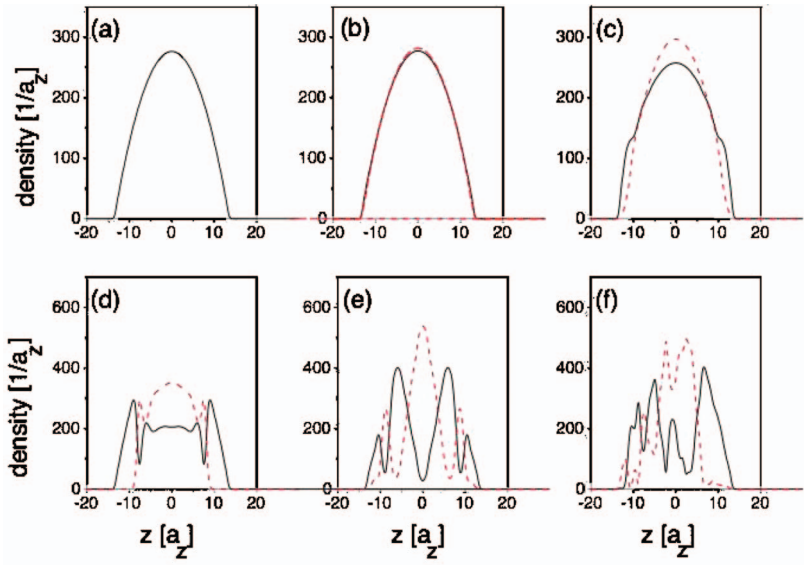

FIG. 3. (Color online) Condensate density of ground state (solid curve) and excited state (dashed curve) components for the interstate two-particle correlation parameter at zero separation $\alpha_{12}^{(2)}=1$, after the first $\pi/2$ pulse for a sequence of interpulse times (a) $T=0$ s, (b) $T=0.36$ s, (c) $T=1$ s, (d) $T=2$ s, (e) $T=50$ s, and (f) $T=220$ s. At $T=0$ s the two spin components have the same amplitude since the microwave pulse is very short but dephased of $\pi/2$ for a $\pi/2$ pulse.

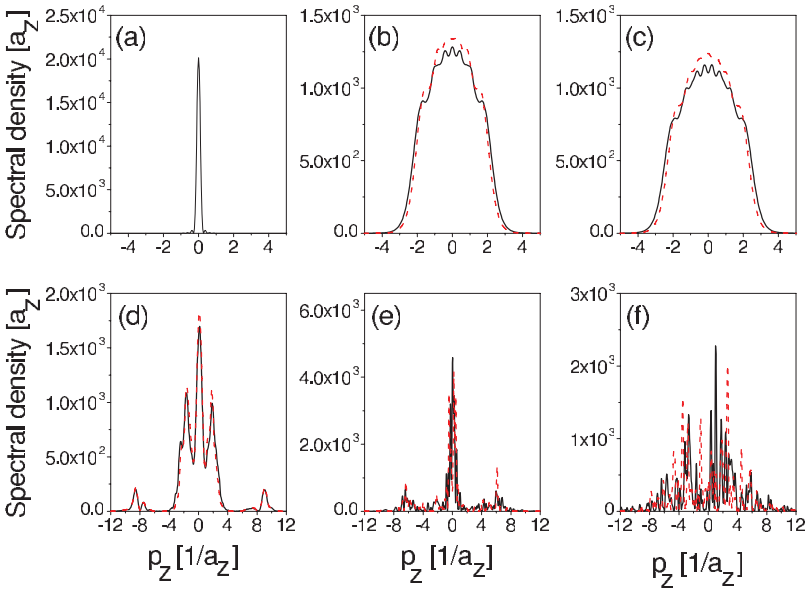

FIG. 4. (Color online) Condensate momentum density of ground (solid curve) and excited (dashed curve) state component for the interstate two-particle correlation parameter at zero separation $\alpha_{12}^{(2)}=2$, after the first $\pi/2$ pulse for a sequence of times (a) $T=0$ s, (b) $T=0.18$ s, (c) $T=0.22$ s, (d) $T=0.26$ s, (e) $T=0.5$ s, and (f) $T=1$ s.

$$c_-^2 = \frac{\hbar^2}{ma_\perp^2}\{\alpha_{11}^{(2)}a_{11}n_1 + \alpha_{22}^{(2)}a_{22}n_2 - \sqrt{(\alpha_{11}^{(2)}a_{11}n_1)^2 + (\alpha_{22}^{(2)}a_{22}n_2)^2 + [2(\alpha_{12}^{(2)}a_{12})^2 - \alpha_{11}^{(2)}\alpha_{22}^{(2)}a_{11}a_{22}]2n_1n_2}\} \tag{9}$$

is the phononlike sound velocity at low momenta. For instability, $c_-^2<0$ and $\Omega_{-,k_f}^2<0$. The fastest growing mode has wave number $k_f=\sqrt{2}m|c_-|/\hbar$, and grows with an initial rate of $m|c_-|^2/\hbar$. Equations (8) and (9) show that the local phase separation of the two condensate components and the symmetry breaking are due to the cross interaction terms under the condition $c_-^2<0$ which occurs when $(\alpha_{12}^{(2)}a_{12})^2 > \alpha_{11}^{(2)}\alpha_{22}^{(2)}a_{11}a_{22}/2$. Equation (9) shows that the time at which the symmetry breaking starts depends on the atomic density; the higher the density (corresponding to larger parameter $|c_-|$), the smaller the symmetry breaking appearance time. We obtain a value of $\tau_{ps}=35$ ms which is smaller than the time from which the phase separation starts in Fig. 2. This discrepancy is probably due to the space-dependent atomic density that locally changes the value of τ_{ps}, increasing from the center of the clouds where the density is higher to the edge where the density is smaller. As the instability depends on the density of atoms, the local spiked structures start to develop at the center of the trap and then spread throughout the clouds.

Note that the case of $\alpha_{12}^{(2)}=1$ with the same numerical parameters values yields $\tau_{ps}\approx 7$ s and the numerical calculation yields a value beyond 120 s for the appearance of the symmetry breaking (Fig. 6). In this case, the phase separation appears much earlier, ≈ 0.4 s before the symmetry breaking takes place. Indeed as the intrastate and interstate interaction strengths are almost identical, the BEC clouds are not strongly perturbed after the first $\pi/2$ pulse. Hence, the two BEC components are barely unstable and phase separation and the symmetry breaking does not occur until much later than in the case of $\alpha_{12}^{(2)}=2$. This clearly increases the stability of the clock. The smaller the difference between the interstate and intrastate interaction strength, the longer the interrogation time and the higher the stability of the clock.

The spiked structure and phase separation in position space is correlated with a delocalization in momentum space created by the strong excitation of the two BEC components as the dynamics proceeds. Indeed the calculated density of the atoms in momentum space is completely delocalized beyond 0.5 s, as shown in Fig. 4. The increased width of the momentum distribution observed from $t=0$ s to $t=0.22$ s is due to the fact that after the first $\pi/2$ pulse the interaction energy converts to the kinetic energy. To monitor the symmetry breaking shown in Fig. 1(d), we calculate the mean value of the axial momentum of each spin component as a function of time, $\langle p_{i_z}(t)\rangle = \int p_{i_z}(t)|\psi_i(p_z,t)|^2 dp_z$, where $\psi_i(p_z,t)$ is the Fourier transform of the condensate wave function $\psi_i(z,t)$. Figure 5 shows the evolution of the mean value of momentum of the two condensates as a function of time. The mean value of the momentum for each spin component is zero from 0 to 0.24 s, and then the mean momentum of each component starts oscillating in time, but the total momentum is conserved. We note that the symmetry breaking appears after the density starts showing an irregular profile of small amplitude at its center. Comparison of Fig. 5 and Fig. 6 shows that phase separation occurs at much later times.

We now analyze the effect of the mean-field dynamics of the system on the performance of the clock. Figure 7 shows the calculated probability P_e for finding atoms in the excited state immediately after the second $\pi/2$ Ramsey pulse as a function of the detuning $\Delta\nu$ of the microwave frequency from the atomic transition frequency times the interrogation time, $\Delta\nu T$. The curves in Fig. 7(a) have been calculated for three values of the interrogation time, $T=0.18$ s (solid

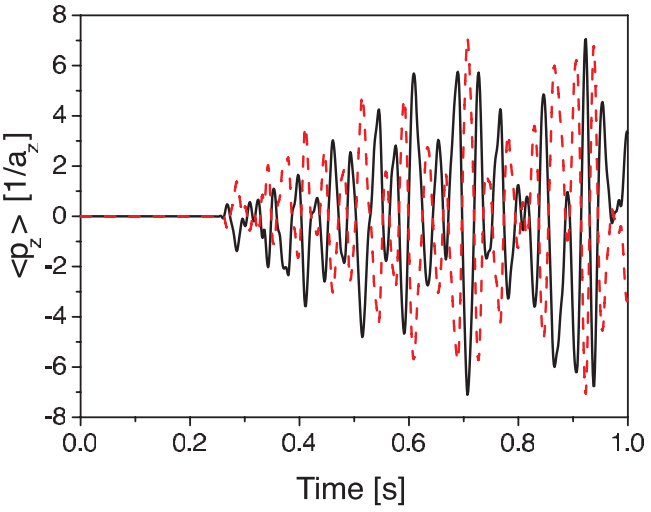

FIG. 5. (Color online) Evolution of the mean value of the momentum of ground (solid curve) and excited (dashed curve) state component after the first $\pi/2$ pulse as a function of time for $\alpha_{12}^{(2)}=2$.

curve), 0.5 s (dashed curve), and 1 s (dotted curve). The fringe contrast decreases as the interrogation time increases. Figure 7(b) plots the variance of the excited population $NP_e(1-P_e)$ [30,31]. The variance is large at time $T=0.5$ and 1.0 s where the condensate profiles are spiked and asymmetrical, and this results in poor stability of the clock. The interrogation time of $T=0.18$ s where the condensates show a smooth and symmetrical profile lead to a frequency stability of $2.6\times10^{-12}\sqrt{T_c/\tau}$ where T_c is the cycle period and τ the averaging time. It is important to note that the stability can be improved by further decreasing the axial and radial frequencies, keeping a high anisotropy ratio so that the quasi-1D regime remains. The improvement will depend on how low the axial frequency can be made without causing fluctuations of the trapping magnetic field. The goal is to further lower the density so as to increase the time at which the phase separation of the two spin components after the first microwave pulse, and hence increase the interrogation

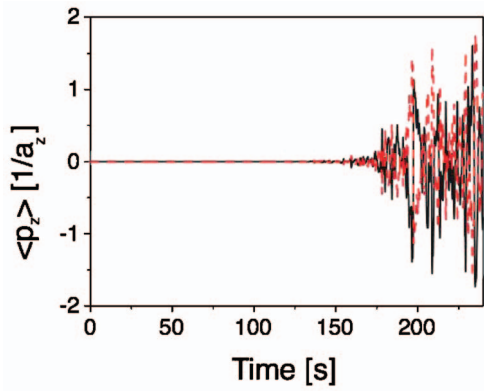

FIG. 6. (Color online) Evolution of the mean value of the momentum of ground (solid curve) and excited (dashed curve) state component after the first $\pi/2$ pulse as a function of time for $\alpha_{12}^{(2)}=1$.

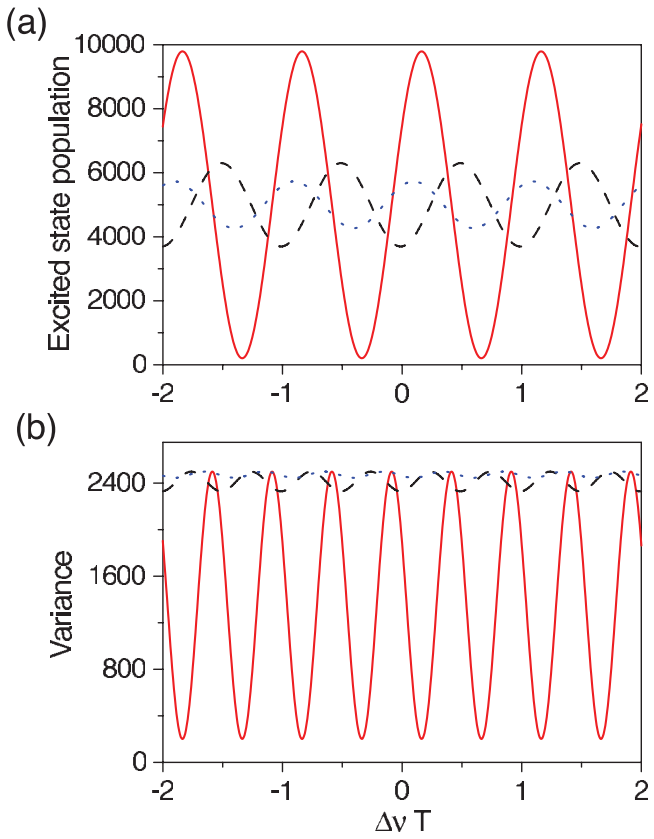

FIG. 7. (Color online) Excited state population (a) and it variance (b) as a function of $\Delta\nu T$, for a sequence of interpulse times: $T=0.18$ s (solid curve), $T=0.5$ s (dashed curve), and $T=1$ s (dotted curve) for $\alpha_{12}^{(2)}=2$.

time. The total number of atoms can also be independently optimized. Thus, it will hopefully be possible to reach a stability beyond $10^{-12}\sqrt{T_c/\tau}$.

We can express the Allan standard deviation for a Ramsey fringe experiment as $\sigma=\frac{1}{\pi\nu_0 T\sqrt{N}}\sqrt{T_c/\tau}$, as a function of the axial trapping frequency. The interrogation time is fixed by the density of the atoms; the higher the density, the smaller the interrogation time. By fixing the interrogation time T_{fix} to correspond to a given density of atoms $n=N/l_z$, where $l_z=(3g_{11}^{1D}N/2m\omega_z^2)^{1/3}$, it is possible to vary the number of atoms and the axial frequency. By equating the density calculated for a different number of atoms and trap frequency, we derive the number of the atoms as a function of the axial trapping frequency,

$$N=N_{\mathrm{fix}}\frac{\omega_{z,\mathrm{fix}}}{\omega_z}, \tag{10}$$

where N_{fix} and $\omega_{z,\mathrm{fix}}$ are, respectively, the given number of atoms and axial trapping frequency that fix the density and the interrogation time T_{fix}. Then the Allan standard deviation is

$$\sigma(\omega_z)=\frac{1}{\pi\nu_0 T_{\mathrm{fix}}\sqrt{N_{\mathrm{fix}}}}\left(\frac{\omega_z}{\omega_{z,\mathrm{fix}}}\right)^{1/2}\sqrt{T_c/\tau}, \tag{11}$$

and varies as the square root of the axial trapping frequency. In our case, using $N_{\mathrm{fix}}=10^4$ atoms and $\omega_{z,\mathrm{fix}}=0.5$ Hz, we find

$T_{\rm fix}=180$ ms for $\alpha_{12}^{(2)}=2$, and the values of the interrogation time obtained by varying the axial trapping frequency are within about 10% of $T_{\rm fix}$.

The projection noise does not have a simple expression as a function of the radial frequency because the instability of the BEC depends both on the density and the geometry of the cloud. Furthermore, the variation of the radial frequency deeply affects the geometry of the cloud and changes the interaction strength $g_{11}^{\rm 1D}$.

Normally we should add to the projection noise, the frequency noise due to the fluctuation of the density introduced by the fluctuation of the total number of atoms. However, as we shall see in the next section, there is a simple method to cancel the collisional frequency shift and then the noise due to density fluctuations will cancel too.

IV. IMPROVEMENT OF THE CLOCK: CANCELLATION OF THE COLLISIONAL SHIFT

In this section we analyze the possibility of improving the clock by cancelling the collisional shift. One of the advantages resulting from the cancellation of the collisional shift is that the clock becomes insensitive to the variation of the total number of atoms. Indeed, even if the density is low, nevertheless the variation of the total number of atoms at each cycle period creates a variation of the density of the atoms and this introduces noise that limits the stability of the clock. As the collisional frequency shift depends on the density of atoms, the idea is to cancel the collisional shift so that such a variation of the density of atoms does not affect the stability of the clock. Note that the variation of the number of atoms we are referring to is not due to quantum fluctuations but rather due to experimental fluctuations in the number of atoms. Here we present two different proposals to overcome this problem.

A small density of atoms in the excited state minimizes the collisional dipolar relaxation loss. But the clock sensitivity to quantum fluctuations increases if the population of atoms in the excited state is too small. So an optimization of the density of atoms is necessary to obtain both good signal-to-noise ratio and a long clock time, yet having small collisional dipolar relaxation. We can use the Zeeman shift to compensate the collisional shift. This method can be applied both to a normal cold atomic cloud and a BEC, and has been proposed in Ref. [8]. However, this method requires adjusting two parameters and seems not to be simple to implement. We will not use it in this paper. Instead, we study the cancellation of the collisional shift terms by playing them off against each other as discussed by Gibble and Verhaar in Ref. [11] for a thermal cesium atom clock. The expression for the collisional frequency shift is [8,11,25,32–34]

$$\Delta\nu_{\rm int}=\frac{\hbar}{m\pi a_\perp^2}(\alpha_{12}^{(2)}a_{12}n_1+\alpha_{22}^{(2)}a_{22}n_2-\alpha_{11}^{(2)}a_{11}n_1-\alpha_{12}^{(2)}a_{12}n_2), \tag{12}$$

where n_1 and n_2 are the density of atoms per unit length in the ground and excited state, respectively. By equating $\Delta\nu_{\rm int}$ to zero, we obtain a simple relation between the density of the atoms in the two states,

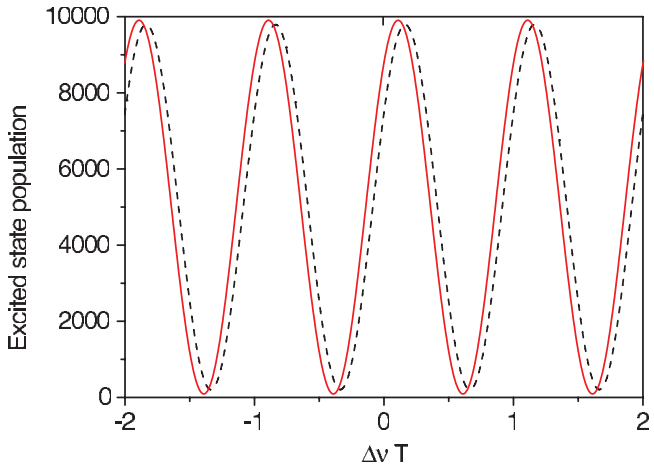

FIG. 8. (Color online) Excited state population as a function of the detuning $\Delta\nu$ of the microwave pulse from atomic transition times the interrogation time in the presence (dashed curve) or without collision (solid curve) for an interpulse time $T=0.18$ s, and the interstate two-particle correlation at zero separation $\alpha_{12}^{(2)}=2$.

$$\frac{n_2}{n_1}=\frac{\alpha_{12}^{(2)}a_{12}-\alpha_{11}^{(2)}a_{11}}{\alpha_{12}^{(2)}a_{12}-\alpha_{22}^{(2)}a_{22}}. \tag{13}$$

The above relation is satisfied only if $\alpha_{12}^{(2)}>\alpha_{11}^{(2)}a_{11}/a_{12}$ and $\alpha_{12}^{(2)}>\alpha_{22}^{(2)}a_{22}/a_{12}$, or $\alpha_{12}^{(2)}<\alpha_{11}^{(2)}a_{11}/a_{12}$ and $\alpha_{12}^{(2)}<\alpha_{22}^{(2)}a_{22}/a_{12}$. When $\alpha_{11}^{(2)}=\alpha_{22}^{(2)}=1$, and a_{12} is only slightly different from a_{11} and a_{22}, such that $a_2<a_{12}<a_{11}$, the cancellation of the collisional shift is possible only for $\alpha_{12}^{(2)}\geqslant 1.02$ or $\alpha_{12}^{(2)}\leqslant 0.97$. For $\alpha_{12}^{(2)}=1$ the ratio n_2/n_1 in Eq. (13) is negative, and therefore cancellation of the collisional shift is not possible. For the scattering lengths of ^{87}Rb and $\alpha_{12}^{(2)}=2$, the density ratio is $n_2=0.95n_1$. Such a ratio should maintain the sizes of the two components to be almost identical. For a ratio of densities close to unity, the Zeeman frequency shift terms due to the size of the atomic clouds will be small. However, a problem originates from $|2\rangle$-$|2\rangle$ collisional dipolar relaxation which can be important at high density and this can limit the clock run time. But in a quasi-1D system, the inelastic ultracold collisions are further reduced. To illustrate the improvement of collisional shift, Fig. 8 shows the calculated excited state population as a function of $\Delta\nu T$ for an interpulse time $T=0.18$ s. The dashed curve is for the case of $\pi/2$ pulses and the solid curve shows the case of the slightly different populations suggested above. In the latter case, the collisional shift is cancelled and this gives a better fringe contrast and a smaller frequency shift. The improvement of fringe amplitude is due to the fact that the difference in the phase of the condensates is space independent as the collisional shift is cancelled.

The remaining frequency shift is now due to kinetic and Zeeman shift. The frequency shift due to the kinetic term,

$$\Delta\nu_{\rm kinetic}=\frac{\langle p_z^2\rangle_2-\langle p_z^2\rangle_1}{4\pi m\hbar}, \tag{14}$$

is -10.997 Hz and the shift due to the Zeeman terms,

$$\Delta\nu_{\text{Zeeman}} = \frac{\langle m\omega_z^2 z^2\rangle_2 - \langle m\omega_z^2 z^2\rangle_1}{4\pi\hbar}, \tag{15}$$

is −0.266 Hz, giving a total frequency shift of $\Delta\nu = -11.263$ Hz, in good agreement with the frequency shift 11.12 Hz determined from the interference pattern of the solid curve in Fig. 8. In Eqs. (14) and (15), the symbol $\langle\cdots\rangle_i$ denotes the expectation value calculated with the wave function $\psi_i(t=T)$. We see that the shift introduced by the Zeeman terms is small because it is proportional to the difference of the square of the size of each condensate and this difference is small. The shift due to the kinetic terms is proportional to the difference of the square of the width of the spectral density of each condensate. As the size of the condensates and the width of their spectral density change in time, the shifts are time dependent.

V. CONCLUSION

We modeled a microwave frequency atomic clock using a configuration of BEC atoms in a highly elongated magnetic trap. We showed that the stability of the clock for a trap radial frequency $\omega_r/2\pi = 120$ Hz and axial frequency $\omega_z/2\pi = 0.5$ Hz is $2.6\times10^{-12}\sqrt{T_c/\tau}$ and $1\times10^{-12}\sqrt{T_c/\tau}$ for $\alpha_{12}^{(2)}=2$ and $\alpha_{12}^{(2)}=1$, respectively. The performance of the clock is related to the configuration of the trap and can be improved by running the clock with an even weaker axial trapping frequency. We found a dynamical instability that results in phase separation and limits the clock stability and accuracy if a long interrogation time is used depending on the density of atoms and on the ratio between the intrastate and interstate two-particle correlation parameter at zero separation. We considered that optimization of the experimental parameters maximize the stability and accuracy of the clock. For a ^{87}Rb BEC, collisional shift terms can be cancelled by playing them off against each other by adjusting the population in the ground and excited states with the Ramsey pulses so that the problem of density fluctuations does not strongly affect the stability and the accuracy of the clock. This can be done only if the two-particle correlation parameters satisfy the relations $\alpha_{12}^{(2)} > \alpha_{11}^{(2)} a_{11}/a_{12}$ and $\alpha_{12}^{(2)} > \alpha_{22}^{(2)} a_{22}/a_{12}$, or $\alpha_{12}^{(2)} < \alpha_{11}^{(2)} a_{11}/a_{12}$ and $\alpha_{12}^{(2)} < \alpha_{22}^{(2)} a_{22}/a_{12}$. The equality of these previous relations automatically cancel the collisional shift.

ACKNOWLEDGMENTS

The authors thank R. Tasgal and Y. Japha for useful conversations. This work was supported in part by grants from the U.S.-Israel Binational Science Foundation (Grant No. 2002147), the Israel Science Foundation for a Center of Excellence (Grant No. 8006/03), and the German Federal Ministry of Education and Research (BMBF) through the DIP project.

[1] M. Takamoto and H. Katori, Phys. Rev. Lett. **91**, 223001 (2003).
[2] H. Katori, M. Takamoto, V. G. Palchikov, and V. D. Ovsiannikov, Phys. Rev. Lett. **91**, 173005 (2003).
[3] R. Folman, P. Krueger, J. Schmiedmayer, J. Denschlag, and C. Henkel, Adv. At., Mol., Opt. Phys. **48**, 263 (2002).
[4] H. Ott, J. Fortagh, G. Schlotterbeck, A. Grossmann, and C. Zimmermann, Phys. Rev. Lett. **87**, 230401 (2001); W. Hänse, P. Hommelhoff, T. W. Hänsch, and J. Reichel, Nature (London) **413**, 498 (2001).
[5] P. Treutlein, P. Hommelhoff, T. Steinmetz, T. W. Hansch, and J. Reichel, Phys. Rev. Lett. **92**, 203005 (2004).
[6] S. Knappe, V. Shah, P. D. D. Schwindt, L. Hollberg, J. Kitching, L. A. Liew, and J. Moreland, Appl. Phys. Lett. **85**, 1460 (2004); S. Knappe, P. D. D. Schwindt, V. Shah, L. Hollberg, J. Kitching, L. Liew, and J. Moreland, Opt. Express **13**, 1249 (2005); S. Knappe, V. Gerginov, P. Schwindt, V. Shah, L. Hollberg, and J. Kitching, Opt. Lett. **30**, 2351 (2005).
[7] N. Ramsey, Phys. Rev. **78**, 695 (1950); N. Ramsey, *Molecular Beams* (Oxford University Press, Oxford, 1985).
[8] D. M. Harber, H. J. Lewandowski, J. M. McGuirk, and E. A. Cornell, Phys. Rev. A **66**, 053616 (2002).
[9] V. A. Yurovsky and Y. B. Band, e-print physics/0602181.
[10] Clearly, in a magnetic field, the only good quantum numbers are m_f. In the presence of a magnetic field, what we mean by states $|f,m_f\rangle$ are the states $|m_f\rangle$ that correlate at zero field to $|f,m_f\rangle$.
[11] K. Gibble and B. J. Verhaar, Phys. Rev. A **52**, 3370 (1995).
[12] C. Fertig and K. Gibble, Phys. Rev. Lett. **85**, 1622 (2000).
[13] Y. Sortais, S. Bize, C. Nicolas, A. Clairon, C. Salomon, and C. Williams, Phys. Rev. Lett. **85**, 3117 (2000).
[14] D. S. Hall, M. R. Matthews, J. R. Ensher, C. E. Wieman, and E. A. Cornell, Phys. Rev. Lett. **81**, 1539 (1998).
[15] Tin-Lun Ho and V. B. Shenoy, Phys. Rev. Lett. **77**, 3276 (1996).
[16] H. Pu and N. P. Bigelow, Phys. Rev. Lett. **80**, 1130 (1998).
[17] E. Timmermans, Phys. Rev. Lett. **81**, 5718 (1998).
[18] M. Trippenbach, K. Goral, K. Rzazewski, B. Malomed, and Y. B. Band, J. Phys. B **33**, 4017 (2000).
[19] J. Vanier and C. Audoin, *The Quantum Physics of Atomic Frequency Standards* (Adam Hilger, IOP, Bristol, 1989), Chap. 5.
[20] Y. B. Band and A. Vardi, Phys. Rev. A **74**, 033807 (2006).
[21] Y. B. Band, J. P. Burke, A. Simoni, and P. S. Julienne, Phys. Rev. A **64**, 023607 (2001); Y. B. Band, M. Trippenbach, J. P. Burke, and P. S. Julienne, Phys. Rev. Lett. **84**, 5462 (2000).
[22] W. Ketterle and H.-J. Miesner, Phys. Rev. A **56**, 3291 (1997).
[23] M. W. Zwierlein, Z. Hadzibabic, S. Gupta, and W. Ketterle, Phys. Rev. Lett. **91**, 250404 (2003).
[24] K. V. Kheruntsyan, D. M. Gangardt, P. D. Drummond, and G. V. Shlyapnikov, Phys. Rev. Lett. **91**, 040403 (2003).
[25] M. Naraschewski and R. J. Glauber, Phys. Rev. A **59**, 4595 (1999).
[26] E. A. Cornell (private communication).
[27] M. Olshanii, Phys. Rev. Lett. **81**, 938 (1998).
[28] Y. B. Band and M. Trippenbach, Phys. Rev. A **65**, 053602 (2002).

[29] A. Smerzi, A. Trombettoni, P. G. Kevrekidis, and A. R. Bishop, Phys. Rev. Lett. **89**, 170402 (2002).
[30] W. M. Itano, J. C. Bergquist, J. J. Bollinger, J. M. Gilligan, D. J. Heinzen, F. L. Moore, M. G. Raizen, and D. J. Wineland, Phys. Rev. A **47**, 3554 (1993).
[31] D. J. Wineland, J. J. Bollinger, W. M. Itano, and D. J. Heinzen, Phys. Rev. A **50**, 67 (1994).
[32] J. M. V. A. Koelman, S. B. Crampton, H. T. C. Stoof, O. J. Luiten, and B. J. Verhaar, Phys. Rev. A **38**, 3535 (1988).
[33] M. O. Oktel, T. C. Killian, D. Kleppner, and L. S. Levitov, Phys. Rev. A **65**, 033617 (2002).
[34] E. Tiesinga, B. J. Verhaar, H. T. C. Stoof, and D. van Bragt, Phys. Rev. A **45**, R2671 (1992).